



Cite this: *Dalton Trans.*, 2015, **44**, 3720

Received 3rd December 2014,  
Accepted 19th January 2015

DOI: 10.1039/c4dt03698k

www.rsc.org/dalton

## The new triazine-based porous copper phosphonate $[\text{Cu}_3(\text{PPT})(\text{H}_2\text{O})_3]\cdot 10\text{H}_2\text{O}^\dagger$

N. Hermer and N. Stock\*

High throughput methods were employed in the discovery of  $[\text{Cu}_3(\text{PPT})(\text{H}_2\text{O})_3]\cdot 10\text{H}_2\text{O}$  (denoted CAU-14). The structure contains one-dimensional channels with a diameter of 9.4 Å. Thermal activation leads to the formation of uncoordinated metal sites and a high water uptake of 39.1 wt% was found.

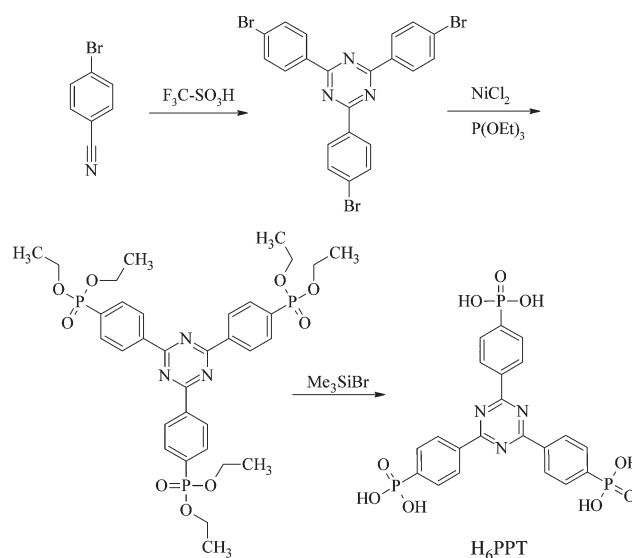
In the intensely investigated field of porous crystalline materials metal organic frameworks offer exceptional properties, such as unsaturated metal sites in the pores. The comparatively high surface areas and the possibility of incorporating different functional groups lead to many potential applications including gas storage, separation, drug delivery and catalysis.<sup>1</sup> For these applications stability is crucial. Most metal organic frameworks built of carboxylate-based linker molecules are often not stable against moisture or temperature. A way to form more stable compounds is to use phosphonate-based linker molecules.<sup>2</sup> The higher charge and larger number of atoms involved in bonding lead to more stable frameworks.<sup>3</sup> A disadvantage of this approach is the tendency of metal phosphonates to form dense layered structures. Thus the number of known porous metal phosphonates is very limited (Table S1†).

Different approaches have been used to form porous metal phosphonates. One strategy to introduce porosity in layered metal phosphonates involves the use of large linear diphosphonic acids in combination with small monophosphonic acids.<sup>4</sup> These materials exhibit low crystallinity and a broad pore size distribution. Another strategy is the use of methylphosphonic acid. This led to the first crystalline porous metal phosphonates  $\text{Cu}(\text{O}_3\text{PCH}_3)$ <sup>5</sup> and  $\beta\text{-Al}_2(\text{O}_3\text{PCH}_3)_3$ .<sup>6</sup> Another strategy is to disrupt the formation of layered structures, for example through the insertion of other functional groups like the amine group that coordinates to the metal ion. An example

is the STA-12 family with the composition  $[\text{M}_2(\text{H}_2\text{O})_2(\text{O}_3\text{PCH}_2\text{NC}_4\text{H}_8\text{NCH}_2\text{PO}_3)]\cdot x\text{H}_2\text{O}$ , M = Mg, Mn, Fe, Co, Ni.<sup>7</sup>

In our approach we aim at disrupting the formation of layered structures through the choice of the linker molecule geometry. This approach has very recently been shown to lead to the permanently porous MOFs  $[\text{Zr}_3(\text{O}_9\text{P}_3\text{C}_{24}\text{H}_{18})_4]$ <sup>8</sup> and  $[\text{Al}(\text{O}_9\text{P}_3\text{C}_{12}\text{H}_{18})(\text{H}_2\text{O})]$ .<sup>9</sup>

The new linker molecule employed in this study is 2,4,6-*tri*-(phenylene-4-phosphonic acid)-*s*-triazine ( $\text{H}_6\text{PPT}$ ). It was synthesised in a three step reaction (see Scheme 1). First 2,4,6-*tri*-(4-bromophenyl)-*s*-triazine was obtained by cyclotrimerization of 4-bromobenzonitrile,<sup>10</sup> which was converted by reaction with triethylphosphite and nickel chloride as the catalyst to 2,4,6-*tri*-(4-diethylphosphonophenyl)-*s*-triazine.<sup>11</sup> The ester was converted into 2,4,6-*tri*-(phenylene-4-phosphonic acid)-*s*-triazine ( $\text{H}_6\text{PPT}$ , 1) using  $\text{Me}_3\text{SiBr}$  and  $\text{CH}_3\text{OH}$ .<sup>12</sup>



**Scheme 1** Synthesis of 2,4,6-*tri*-(phenylene-4-phosphonic acid)-*s*-triazine ( $\text{H}_6\text{PPT}$ ).

Christian-Albrechts-Universität, Max-Eyth-Straße 2, 24118 Kiel, Germany.

E-mail: stock@ac.uni-kiel.de; Fax: +49 431 8801775; Tel: +49 431 8803261

† Electronic supplementary information (ESI) available: Details of the high-throughput experiments, the detailed synthesis and characterization of  $\text{H}_6\text{PPT}$  and CAU-14. CCDC 1029260 for CAU-14. For ESI and crystallographic data in CIF or other electronic format see DOI: 10.1039/c4dt03698k



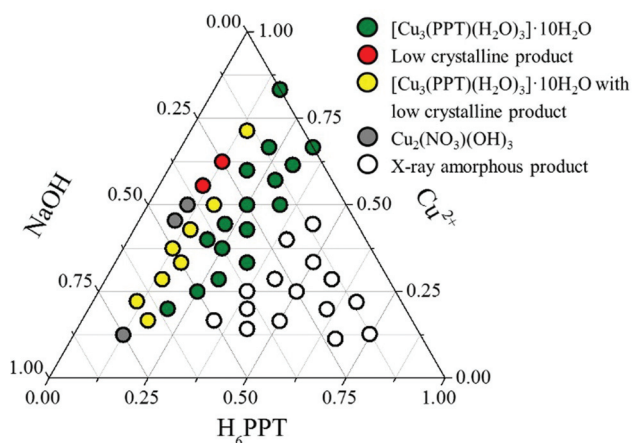


**Fig. 1** Crystallisation diagram of the system  $\text{Cu}^{2+}/\text{H}_6\text{PPT}/\text{NaOH}$ . Each point in the diagram corresponds to a distinct molar ration of the three starting materials.

The system  $\text{Cu}^{2+}/\text{H}_6\text{PPT}/\text{NaOH}$  in water as the solvent was investigated using high-throughput methods.<sup>13</sup> These allow a systematic and efficient investigation of reaction parameters. The investigated molar ratios of the starting materials and the results of the PXRD measurements are shown in the crystallization diagram (Fig. 1, Fig. S1, Table S2†).

CAU-14 is obtained in a Teflon-lined autoclave ( $V_{\text{max}} = 2$  mL) by reaction of a mixture of aqueous 2 M  $\text{Cu}(\text{NO}_3)_2$  (63.7  $\mu\text{L}$ , 0.127 mmol),  $\text{H}_6\text{PPT}$  (70 mg, 0.127 mmol), aqueous 2 M  $\text{NaOH}$  (223  $\mu\text{L}$ , 0.446 mmol) and 713  $\mu\text{L}$  deionised water. The reactor was slowly heated within 16 h to 190 °C. The temperature was kept for 24 h and the reactor was subsequently cooled to room temperature within 24 hours. The precipitate was filtered of and washed with water.

During the synthesis optimisation single crystals of CAU-14 were obtained. Due to the small size of the single crystals (*ca.*  $50 \times 10 \times 10 \mu\text{m}^3$ ) synchrotron radiation was used for single crystal X-ray diffraction. Data was recorded at beamline I19 at the Diamond Light Source in Didcot, UK. The Crystal data and final results of the structure refinement are provided in Table 1, Tables S3, S4, S5.† The asymmetric unit is shown in Fig. 2.

In the structure of CAU-14 each  $\text{Cu}^{2+}$  ion exhibits a distorted square pyramidal coordination environment consisting of four oxygen atoms of four different phosphonate groups

**Table 1** Crystal data for CAU-14

Formula sum	$\text{C}_{21}\text{H}_{12}\text{Cu}_3\text{N}_3\text{O}_{15}\text{P}_3$
Crystal system	Monoclinic
$a/\text{\AA}$ , $b/\text{\AA}$ , $c/\text{\AA}$	25.618(5), 17.040(3), 4.4322(9)
$\beta/^\circ$	99.96(3)
$V/\text{\AA}^3$	1905.6(7)
Space group	$Cm$
Tot., uniq. data, $R_{\text{int}}$	7534, 2946, 0.0596
Observed data [ $I > 2\sigma(I)$ ]	2773
$R_1$ , $wR_2$ (all data)	0.0532, 0.1521
GOF	1.091

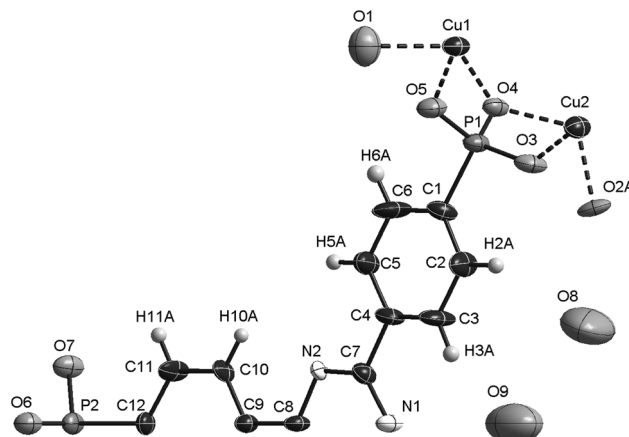


**Fig. 2** The asymmetric unit of CAU-14.

and one coordinated water molecule. Corner-sharing of the  $\text{CuO}_5$  polyhedra leads to the formation of trimeric  $\text{Cu}_3\text{O}_9(\text{H}_2\text{O})_3$  units (Fig. 3a). These units are connected *via* phosphonate groups to form one-dimensional inorganic building units (Fig. 3b). Each column is connected to six adjacent ones *via* the linker molecules (Fig. 3c). This leads to a honeycomb network with pores of approximately 9.4  $\text{\AA}$  in diameter (Fig. 4). Non-coordinating water molecules in the pores partially interact with the nitrogen atoms of the triazine ring through H-bonding interactions (Table S4†).

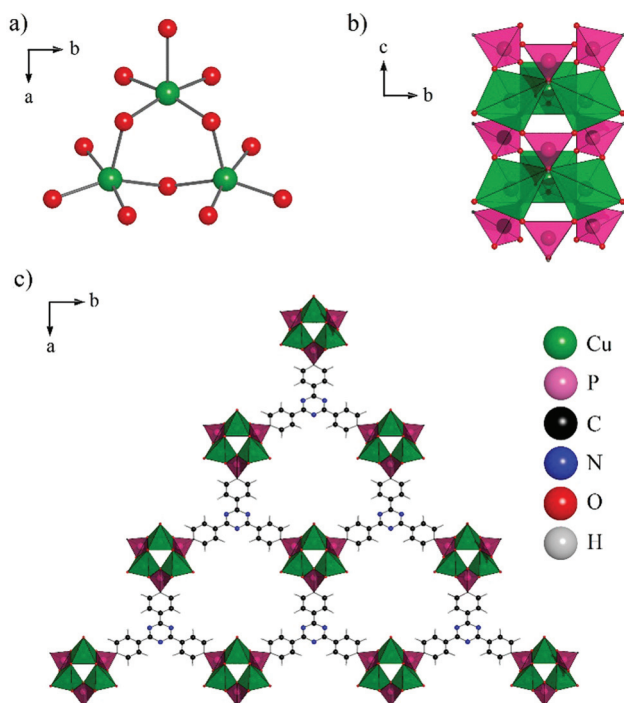


**Fig. 3** (a) The trimeric  $\text{Cu}_3\text{O}_9(\text{H}_2\text{O})_3$  unit, (b) the copper phosphonate pillars viewed down the  $a$ -axis. (c) View along the  $c$ -axis of CAU-14 (water molecules in the pores omitted for clarity).  $\text{CuO}_5$  and  $\text{CPO}_3$  polyhedra are shown in green and red, respectively.



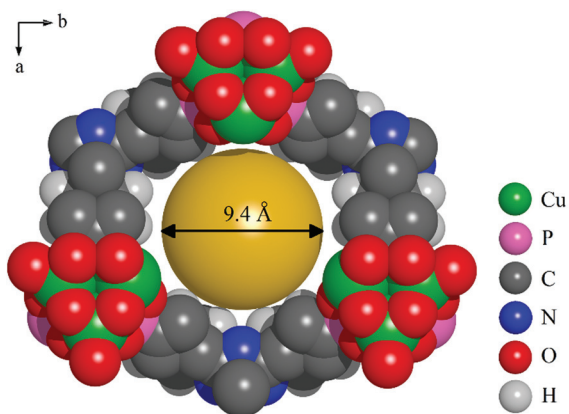


Fig. 4 Space filling view of one pore of CAU-14 along the *c*-axis. A sphere of 9.4 Å in diameter is added to demonstrate the pore size. Water molecules in the pores are omitted for clarity.

Thermogravimetric measurements (Fig. S2†) showed a weight loss up to 150 °C due to the loss of solvent molecules. The framework of CAU-14 is stable up to 380 °C in air. Hence it was activated prior to the sorption experiments at 150 °C for 18 h under reduced pressure ( $10^{-2}$  kPa). Evaluation of the  $N_2$  sorption isotherm (Fig. S3†), recorded at 77 K, lead to a specific surface area of  $a_{\text{BET}} = 647 \text{ m}^2 \text{ g}^{-1}$  and a micropore volume of  $V_{\text{mic}} = 0.27 \text{ cm}^3 \text{ g}^{-1}$  (theoretical micropore volume  $V_{\text{mic}} = 0.37 \text{ cm}^3 \text{ g}^{-1}$ ). CAU-14 is also porous towards  $\text{CO}_2$  (uptake of  $1.1 \text{ mmol g}^{-1}$  (4.84 wt%) at 100 kPa) and  $\text{H}_2$  (uptake of  $3.3 \text{ mmol g}^{-1}$  (0.67 wt%) at 100 kPa) (Fig. S4 and S5†). Stability of CAU-14 was demonstrated by PXRD measurements. A comparison of the PXRD patterns of as-synthesized CAU-14 and CAU-14 after the sorption measurements with a simulated PXRD pattern is given in Fig. S6.†

The activation leads also to the removal of the coordinated water molecules, leaving the framework with unsaturated open metal sites. This was confirmed by the results of the water sorption measurement (Fig. 5) and the colour change of the sample from light to dark green (Fig. 6). The water vapour isotherm shows two distinct steps; first three water molecules per formula sum are adsorbed up to  $p/p_0 = 0.05$ , which corres-

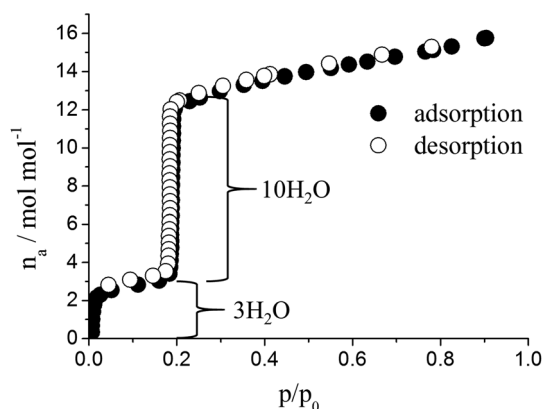


Fig. 5 Water sorption isotherm of CAU-14, measured at 298 K.

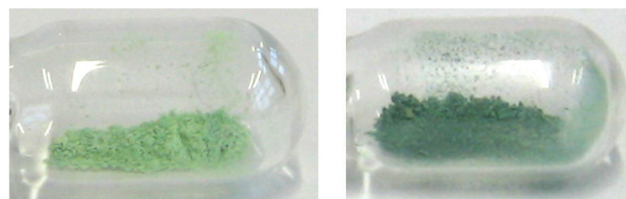


Fig. 6 left: CAU-14 as synthesised, right thermally activated CAU-14.

ponds to the three coordinated water molecules. Around  $p/p_0 = 0.2$  a steep uptake of ten water molecules per formula sum is observed (23.1 wt%). The water sorption is fully reversible and the large loading lift lies within a narrow pressure range ( $0.18 \leq p/p_0 \leq 0.20$ ). In addition only a comparatively small hysteresis is observed (Fig. 5).

These properties could make CAU-14 a promising candidate for heat storage and transformation applications with water as working fluid.<sup>14</sup>

## Conclusions

The small number of porous metal phosphonates has been expanded by the new permanently porous metal phosphonate CAU-14, which is thermally stable up to 380 °C and shows reversible water uptake at 25 °C. The trigonal planar shape of the phosphonic acid prevents the formation of metal phosphonate layers and leads to a porous honeycomb network. Hence the use of trigonal linkers seems to be a promising way to obtain porous metal phosphonates. The structure of CAU-14  $[\text{Cu}_3(\text{PPT})(\text{H}_2\text{O})_3] \cdot 10\text{H}_2\text{O}$  was determined by single crystal X-ray diffraction using synchrotron radiation. Permanent porosity was demonstrated by sorption of  $N_2$ ,  $\text{CO}_2$ ,  $\text{H}_2$  and  $\text{H}_2\text{O}$ . The measured porosity towards nitrogen ( $V_{\text{mic}} = 0.27 \text{ cm}^3 \text{ g}^{-1}$ ) is comparable to the well studied porous metal phosphonate STA-12,  $[\text{M}_2(\text{H}_2\text{O})_2(\text{O}_3\text{PCH}_2\text{NC}_4\text{H}_8\text{NCH}_2\text{PO}_3)] \cdot x\text{H}_2\text{O}$ ,  $\text{M} = \text{Mg}, \text{Mn}, \text{Fe}, \text{Co}, \text{Ni}$ . Upon activation the water molecules in CAU-14 which are bonded to the copper can be removed. This leads to a framework with unsaturated metal sites which could be useful for catalytic transformations.

## Acknowledgements

We thank Diamond Light Source for access to beamline I19 (proposal number 9216) that contributed to the results presented here.

## Notes and references

- 1 Themed issue on Metal Organic Frameworks, *Chem. Rev.*, 2012, **112**, 673; Themed issue on Metal Organic Frameworks, *Chem. Soc. Rev.*, 2014, **43**, 5405.
- 2 A. Clearfield and K. Demandis, in *Metal Phosphonate Chemistry: From Synthesis to Applications*, The Royal Society of Chemistry, Cambridge, UK, 2012.



- 3 K. J. Gagnon, H. P. Perry and A. Clearfield, *Chem. Rev.*, 2012, **112**, 1034; G. K. H. Shimizu, R. Vaidhyanathan and J. M. Taylor, *Chem. Soc. Rev.*, 2009, **38**, 1430.
- 4 M. B. Dines, R. E. Cooksey, P. C. Griffith and R. H. Lane, *Inorg. Chem.*, 1983, **22**, 1003; G. Alberti, F. Marmottini, R. Vivani and P. Zappelli, *J. Porous Mater.*, 1998, **5**, 205.
- 5 J. Le Bideau, C. Payen, P. Palvadeau and B. Bujoli, *Inorg. Chem.*, 1994, **33**, 4885.
- 6 K. Maeda, Y. Kiyozumi and F. Mizukami, *Angew. Chem., Int. Ed.*, 1994, **33**, 2335.
- 7 M. T. Wharmby, G. M. Pearce, J. P. S. Mowat, J. M. Griffin, S. E. Ashbrook, P. A. Wright, L.-H. Schilling, A. Lieb, N. Stock, S. Chavan, S. Bordiga, E. Garcia, G. D. Pirngruber, M. Vreeke and L. Gora, *Microporous Mesoporous Mater.*, 2012, **157**, 3.
- 8 M. Taddei, F. Costantino, R. Vivani, S. Sabatini, S.-H. Lim and S. M. Cohen, *Chem. Commun.*, 2014, **50**, 5737.
- 9 S.-F. Tang, J.-J. Cai, L.-J. Li, X.-X. Lv, C. Wang and X.-B. Zhao, *Dalton Trans.*, 2014, **43**, 5970.
- 10 Y. K. Park, S. B. Choi, H. Kim, K. Kim, B.-H. Won, K. Choi, J.-S. Choi, W.-S. Ahn, N. Won, S. Kim, D. H. Jung, S.-H. Choi, G.-H. Kim, S.-S. Cha, Y. H. Jhon, J. K. Yang and J. Kim, *Angew. Chem., Int. Ed.*, 2007, **119**, 8378.
- 11 P. Tavs, *Chem. Ber.*, 1970, **103**, 2428.
- 12 C. E. McKenna and J. Schmidhuser, *J. Chem. Soc., Chem. Commun.*, 1979, 739.
- 13 P. Maniam and N. Stock, in *Metal Phosphonate Chemistry: From Synthesis to Applications*, The Royal Society of Chemistry, 2012, p. 87.
- 14 F. Jeremias, D. Fröhlich, C. Janiak and S. K. Henninger, *New J. Chem.*, 2014, **38**, 1846.

